OncoTargets and Therapy

Dovepress
open access to scientific and medical research

Open Access Full Text Article

ORIGINAL RESEARCH

Green synthesis, characterization, and anticancer activity of hyaluronan/zinc oxide nanocomposite

This article was published in the following Dove Press journal:
OncoTargets and Therapy
26 July 2016
Number of times this article has been viewed

Farideh Namvar[1,2]
Susan Azizi[3]
Heshu Sulaiman Rahman[4–6]
Rosfarizan Mohamad[1,3]
Abdullah Rasedee[4]
Mozhgan Soltani[2]
Raha Abdul Rahim[7]

[1]Institute of Tropical Forestry and Forest Products (INTROP), Universiti Putra Malaysia, UPM Serdang, Selangor, Malaysia; [2]Research Center for Animal Development Applied Biology, Mashhad Branch, Islamic Azad University, Mashhad, Iran; [3]Department of Bioprocess Technology, Faculty of Biotechnology and Biomolecular Sciences, [4]Department of Veterinary Laboratory Diagnosis, Faculty of Veterinary Medicine, Universiti Putra Malaysia, UPM Serdang, Selangor, Malaysia; [5]Department of Clinic and Internal Medicine, College of Veterinary Medicine, University of Sulaimani, [6]Department of Laboratory Medical Sciences, Komar University of Science and Technology, Sulaimani City, Kurdistan Region, Northern Iraq; [7]Department of Cell and Molecular Biology, Faculty of Biotechnology and Biomolecular Sciences, Universiti Putra Malaysia, UPM Serdang, Selangor, Malaysia

Correspondence: Rosfarizan Mohamad; Susan Azizi
Department of Bioprocess Technology, Faculty of Biotechnology and Biomolecular Sciences, University Putra Malaysia, 43400 UPM Serdang, Selangor, Malaysia
Tel +60 3 8946 3455
Fax +60 3 8946 1071
Email farizanmohd@gmail.com; azisusan@gmail.com

Abstract: The study describes an in situ green biosynthesis of zinc oxide nanocomposite using the seaweed *Sargassum muticum* water extract and hyaluronan biopolymer. The morphology and optical properties of the hyaluronan/zinc oxide (HA/ZnO) nanocomposite were determined by Fourier transform infrared spectroscopy, X-ray diffraction, field emission scanning electron microscopy, transmission electron microscopy, and ultraviolet–vis analysis. Electron microscopy and X-ray diffraction analysis showed that the zinc oxide nanoparticles were polydispersed with a mean size of 10.2±1.5 nm. The nanoparticles were mostly hexagonal in crystalline form. The HA/ZnO nanocomposite showed the absorption properties in the ultraviolet zone that is ascribed to the band gap of zinc oxide nanocomposite. In the cytotoxicity study, cancer cells, pancreatic adenocarcinoma (PANC-1), ovarian adenocarcinoma (CaOV-3), colonic adenocarcinoma (COLO205), and acute promyelocytic leukemia (HL-60) cells were treated with HA/ZnO nanocomposite. At 72 hours of treatment, the half maximal inhibitory concentration (IC_{50}) value via the 3-(4,5-dimethylthiazol-2-yl)-2,5-diphenyltetrazolium bromide (MTT) assay was 10.8±0.3 µg/mL, 15.4±1.2 µg/mL, 12.1±0.9 µg/mL, and 6.25±0.5 µg/mL for the PANC-1, CaOV-3, COLO-205, and HL-60 cells, respectively, showing that the composite is most toxic to the HL-60 cells. On the other hand, HA/ZnO nanocomposite treatment for 72 hours did not cause toxicity to the normal human lung fibroblast (MRC-5) cell line. Using fluorescent dyes and flow cytometry analysis, HA/ZnO nanocomposite caused G2/M cell cycle arrest and stimulated apoptosis-related increase in caspase-3 and -7 activities of the HL-60 cells. Thus, the study shows that the HA/ZnO nanocomposite produced through green synthesis has great potential to be developed into an efficacious therapeutic agent for cancers.

Keywords: green synthesis, hyaluronan, zinc oxide nanocomposite, anticancer activity

Introduction

Hybrid polymer/inorganic nanocomposite materials are a combination of polymer and inorganic phase particles, in which at least one phase is in the nanometer range. Polymer nanocomposite materials display enhanced properties, ie, properties which are significantly more than the properties of the sum of the properties of each individual phase. With its unique optical, electronic, medical, and mechanical properties, the hybrid polymer/inorganic nanocomposites are favorable for many applications.[1] In recent years, there has been a lot of research in the development of hybrid polymer/inorganic nanocomposites that have potential applications in biomedical applications. Of particular interest has been the development of hybrid polymer/inorganic nanocomposites comprising of natural biopolymers, such as hyaluronan, with its biological functions and exclusive physicochemical properties, and zinc oxide nanoparticles, which is well known for its biomedical applications and UV shielding ability.[2] HA belongs to a class of glycosaminoglycan and is also recognized as a mucopolysaccharide. It is one

of the major elements of connective tissues, particularly, the dermis and epidermis. Approximately 35% of human HA is in the muscles and skeleton.[3–5] Other parts of the body rich in HA include the vitreous humor, synovial fluid, and umbilical cord. HA is a high-molecular weight unsulfated polysaccharide and depending on the source can range from 10^4 Da to 10^7 Da in mass.[6] This polymer is composed of D-glucuronic acid and *N*-acetyl glucosamine residues connected by β-1-3 and β-1-4 glycosidic links.

HA due to its high water-holding capacity, mucoadhesion, viscoelasticity, nonimmunogenicity, and biocompatibility is ideal for application as a drug delivery system in ophthalmology, orthopedics, rheumatology, and tissue engineering.[7] In cosmetics, the low-molecular weight HA is used as a moisturizer and lubricating agent.[8] High-molecular weight HA can be obtained through the manipulation of bacterial fermentation process. The application of high-molecular weight HA in cosmetics and therapeutics is yet to be determined.[9]

The hybrid polymer/inorganic nanocomposites can be prepared by in situ or ex situ method using either chemical or physical techniques. In the in situ method, the nanoparticles are synthesized while in mixture with the polymers. In the ex situ method, the nanoparticle and polymer matrices are prepared separately, and the nanoparticles are dispersed in the polymers.[10] In the chemical technique, toxic compounds are generally used, and this restricts the application of the polymer nanocomposite from biological and biomedical applications. To overcome the problem of toxicity, an ecological green approach was introduced to the synthesis of the nanoparticles.[11]

Marine algae have long been used in nutrition and traditional medicine because of their richness in lipids, minerals, vitamins, proteins, polysaccharides, and polyphones. The traditional applications of the algae are the treatment of oxidative stress, allergies, inflammation, cancers, hyperlipidemia, hypertension, and thrombosis.[12] The phytochemical components of the algae including hydroxyl, carboxyl, and amino groups could benefit in the production of inorganic nanoparticles.[13]

Nanoparticles are fast becoming promising agents for drug delivery in the treatment of diseases. Currently, there are several nanoparticle delivery systems that have been developed for cancer therapy, including liposomes, polymer–drug conjugates, and micellar formulations.[14] More recently, nanoparticle drug systems are becoming more sophisticated with the incorporation of multifunctional and targeting capabilities that could potentially overcome drug resistance and improve treatment of metastatic diseases.[15]

To the best of our knowledge, this study is a first report on green synthesis of hyaluronan/ZnO nanocomposite (HA/ZnO) for the treatment of cancers. The challenges in developing this drug delivery system include the identification of tumor-specific targeting moieties, integration of these moieties into nanocarriers, and formulation of a delivery system with drug-sustained release properties.

Materials and methods

Materials

Zinc acetate dihydrate ($Zn[Ac]_2{\cdot}2H_2O$) (99%) (Merck) and sodium hydroxide (NaOH) (Sigma-Aldrich Co., St Louis, MO, USA) were of analytical grade. The seaweed *Sargassum muticum* specimens obtained from the seaside regions of Persian Gulf Sea were washed and freeze-dried and milled into powder. The HA polymer was obtained via bacterial fermentation.[9]

Methods

Preparation of HA/ZnO polymer nanocomposite

The HA solution (100 mL, 1.0% w/v) was prepared by solubilizing HA in sodium hydroxide (1.0% w/v) with constant stirring for 1 hour. The nanoparticles were synthesized by suspending 1.0 g of seaweed in 100 mL of distilled water in a 200 mL Erlenmeyer flask heating to 100°C and filtering through a Whatman 41 filter paper to obtain the seaweed extract. The zinc acetate dehydrate (1 mM) aqueous solution was mixed to 50 mL of water extract seaweed and added to HA solution under constant stirring for 2–3 hours at 70°C. A solid nanocomposite product, the HA/ZnO nanocomposite, was obtained from the suspension by centrifugation at 200× *g* (Hettich zentrifugen, 32 R) for 8 minutes, washed with distilled water, and dried for 4 hours at 100°C, before storing in air-tight bottles at room temperature until use.

Characterization of HA/ZnO nanocomposite

X-ray diffraction (XPert Pro) analysis was used to determine phase purity and particle size of dried seaweed powder samples using CuKα radiation (λ=1.542 Å; 40 kV, 30 mA) at ambient temperature. The chemical compositions were analyzed using Fourier transform infrared (FTIR) spectroscopy (Perkin-Elmer 1725X). The size and shape of the nanoparticles were determined using a Hitachi H-7100 transmission electron microscope (TEM) operated at an acceleration voltage of 120 kV. The size distribution and mean size of the nanoparticles were determined by the Sigma-Scan Pro Software (IBM Corporation, Armonk, NY, USA). The field emission scanning electron microscopy (FESEM) was performed using the Philips model JSM-6360LA machine. UV–visible absorption of solution samples was recorded

over the range of 200–800 nm using a UV–vis spectrophotometer, a Lambda 25-Perkin Elmer. The polydispersity index was obtained by dynamic light scattering using the dispersion technology and light scattering system HPPS software v 4.20.

Cell culture condition

The pancreatic adenocarcinoma (PANC-1), ovarian adenocarcinoma (CaOV-3), colonic adenocarcinoma (COLO205), acute promyelocytic leukemia (HL-60), and normal human lung fibroblast (MRC-5) cell lines were purchased from American Type Culture Collection (ATCC) (Manassas, VA, USA). The cells were maintained in RPMI-1640 (ATCC) medium, supplemented with L-glutamine (2 mM), 10% heat-inactivated fetal calf serum (ATCC), 100 units/mL penicillin, and 100 µg/mL streptomycin (Sigma-Aldrich Co.), according to the ATCC protocol, cultured, and grown in 75 cm^2 culture flasks (TPP, Switzerland) in an incubator with humidified atmosphere of 95% air and 5% CO_2 at 37°C (Binder, Germany). The cell cultures were frequently examined under inverted microscope (Micros, Austria) to determine confluency and viability. The ethics committee of Universiti Putra Malaysia does not deem ethics approval necessary for commercially purchased human cell lines.

Cell growth inhibition assay

The antiproliferative effect of 1–100 µg/mL HA/ZnO nanocomposite on cancer and normal cells was determined by the 3-(4,5-dimethylthiazol-2-yl)-2,5-diphenyltetrazolium bromide (MTT) kit (Sigma-Aldrich Co.). Briefly, the cancer cells were allowed to grow in 75 cm^2 cell culture flask (TPP) until 90% confluent, and the cell density was determined using a hemocytometer (Marienfeld, Germany). Then, 100 µL of cell suspension was seeded into each well of the 96-well microculture plates (TPP) each at a concentration of 1×10^5 cells/mL and treated with 100 µL of various concentrations of HA/ZnO nanocomposite. After incubation for 72 hours in a 5% CO_2 incubator at 37°C, 20 µL of 5 mg/mL MTT solution (microculture tetrazolium) (Sigma-Aldrich Co.) in phosphate buffer solution (PBS, pH 7.5) (Sigma-Aldrich Co.) was added to each well, and the plate was covered with aluminum foil and incubated for an additional 4 hours in the dark to allow the metabolically active viable cells to convert water-soluble yellow MTT solution into the water-insoluble purple formazan crystals. Immediately, 100 µL of incubating medium was aspirated. The purple formazan was then dissolved with 100 µL MTT solubilization solution (Sigma-Aldrich Co.) with mixing and shaking (Eppendorf plate shaker, USA) for 5 minutes.[16] The assay was performed in triplicates. The optical density was recorded using an ELISA plate reader (Universal Microplate reader) (Biotech Inc., USA) at 570 nm. The half maximal inhibitory concentration (IC_{50}) value was determined from the absorbance versus concentration curve. All values from the cells treated with HA/ZnO nanocomposite were compared with those treated with the antineoplastic agent, cisplatin (Sigma-Aldrich Co.). Dimethyl sulfoxide (0.1%)-treated cells served as the negative control.

Acridine orange/propidium iodide assay

The HL-60 cell shown to be most susceptible to HA/ZnO nanocomposite was chosen for subsequent analysis. The effect of HA/ZnO nanocomposite on the HL-60 cells was determined using the acridine orange/propidium iodide (AO/PI) double staining method according to standard procedure. The cells were examined under a fluorescence microscope (Leica Microsystems, Wetzlar, Germany) with the Q-floro software installed. The HL-60 cells at a concentration of 1×10^6 cells/mL were placed in a 25 cm^2 culture flask (TPP) and then treated with IC_{50} concentration of HA/ZnO nanocomposites and incubated in a 5% CO_2 incubator for 24 hours, 48 hours, and 72 hours at 37°C. After treatment, the cells were centrifuged at 200× *g* (Hettich zentrifugen, 32 R) for 10 minutes, and the supernatant discarded. The cells were then washed twice with PBS and centrifuged each time at 200× *g* for 10 minutes to remove the medium. Approximately 10 µL of the cell pellets were stained for 2 minutes with 10 µL fluorescent dyes mixture containing equal volumes (100 µg/mL) of AO and PI. Approximately 10 µL of freshly stained cell suspension was placed onto a glass slide, covered with cover slip, and examined under a fluorescence microscope within 30 minutes before the fluorescence began to fade.[17]

Annexin V–fluorescein isothiocyanate

The HL-60 cells at 1×10^6 cells/mL per well were treated with IC_{50} concentration of HA/ZnO nanocomposite for 6 hours, 12 hours, and 24 hours. Untreated cells served as controls. The HL-60 cells suspension was then aspirated and centrifuged at 200× *g* (Hettich zentrifugen, 32 R) for 10 minutes to remove the medium. The cell pellets were washed twice with 1 mL ice-cold PBS, recentrifuged, and resuspended in ice-cold 1× binding buffer. Precisely 500 µL of cell suspension was transferred to a 5 mL culture tube (TPP), to which 5 µL of annexin V–fluorescein isothiocyanate conjugate and 10 µL of PI were added. The cells were incubated for 15 minutes at room temperature in the dark and then subjected to flow cytometric analysis using the BD FACS Calibur flow cytometer (BD, Franklin Lakes, NJ, USA). The data analysis was performed using the CellQuest Pro software.

Cell cycle assay

Flow cytometer analysis was also used to determine the HL-60 cell cytotoxicity of HA/ZnO nanocomposite. Briefly, 2.5×10^6 cells/mL of HL-60 cells were cultured with the IC_{50} concentration of HA/ZnO nanocomposite in each well and incubated for 12 hours, 24 hours, and 48 hours. The cells were harvested by centrifugation at 200× *g* (Hettich zentrifugen, 32 R) for 5 minutes and washed with 1 mL PBS (pH 7.4) containing 0.1% sodium azide. Then 500 µL of 70% ice-cold ethanol was added to the cell pellets drop by drop with constant mixing to prevent clumping and aggregation and kept at –20°C for 1 week. One milliliter of PBS was added, and the suspension was centrifuged at 200× *g* (Hettich zentrifugen, 32 R) for 5 minutes to pellet cells and remove the ethanol. The cell pellets were washed twice with 1 mL PBS and stained with PBS staining buffer that contained 0.1% triton X-100, 10 mM ethylenediaminetetraacetic acid, 50 µg/mL RNAase A, and 3 µg/mL PI and incubated on ice in dark for 30 minutes.[18] Flow cytometric analysis was conducted using the BD FACS Calibur flow cytometer (BD), and data analysis was performed using the CellQuest Pro software.

Caspase assay

To determine if apoptosis is a mode of HL-60 cell death caused by HA/ZnO nanocomposite, the caspase-3 and -9 activities were estimated colorimetrically using the Gene script kit (Piscataway, NJ, USA). Briefly, 1×10^6 HL-60 cells in each well were first treated with HA/ZnO nanocomposite for 24 hours, 48 hours, and 72 hours. The medium was aspirated, and the cells were washed with pre-chilled PBS. Cell lysates were prepared by adding 100 µL lysis buffer to each well and allowing to stand for 20 minutes on ice to complete cell lysis. After centrifugation at 200× *g* (Hettich zentrifugen, 32 R), the supernatants were collected and the protein concentration was quantified by the Bradford assay. The lysates were finally incubated in the dark at 37°C for 4 hours, and the absorption read at 490 nm in an ELISA microplate reader (Biotech Inc., USA).[19]

Statistical analysis

The results were expressed as mean ± standard deviation. The statistical analysis was done using SPSS version 20.0 (IBM Corporation). *P*-values <0.05 were assumed to be significant.

Results and discussion

Characterization of HA/ZnO nanocomposite

Figure 1 illustrates FTIR spectra of (a) HA, (b) *S. muticum*, and (c) HA/ZnO nanocomposite. Spectrum (a) confirmed the presence of HA with bands at 3,412 cm^{-1}, 1,616 cm^{-1}, 1,411 cm^{-1}, 1,149 cm^{-1}, 1,066 cm^{-1}, 946 cm^{-1}, and 661 cm^{-1}.[20] Spectrum (b) represents *S. muticum* with bands at 3,340 cm^{-1}, 1,610 cm^{-1}, 1,420 cm^{-1}, 1,270 cm^{-1}, and 1,037 cm^{-1}.[21,22] Spectrum (c) represents HA/ZnO nanocomposite. The formation of ZnO nanoparticles is confirmed by a band at 441 cm^{-1}. The band at 1,270 cm^{-1} is attributed to the asymmetric sulfate stretching vibration, and the peak at 1,066 cm^{-1} ascribed to symmetric C–O vibration related to a C–O–SO_3[23] or the C–OH had become weak in the formation of ZnO nanoparticles, indicating participation of the sulfate groups on polysaccharides of the *S. muticum* and the hydroxyl groups of both the *S. muticum* and the HA. On the other hand, the peaks at ~1,632 cm^{-1} and 1,433 cm^{-1} correspond to stretching vibration of (NH)C=O and –COO or OH groups, respectively. These peaks became strong and shifted slightly with the synthesis of ZnO nanoparticles, indicating that interactions between the (NH)C=O, –COOH, and OH groups of HA and *S. muticum* and the –OH groups of ZnO nanoparticle surfaces had occurred. These interactions had allowed for the stabilization and capping of ZnO nanoparticles with HA and *S. muticum.*

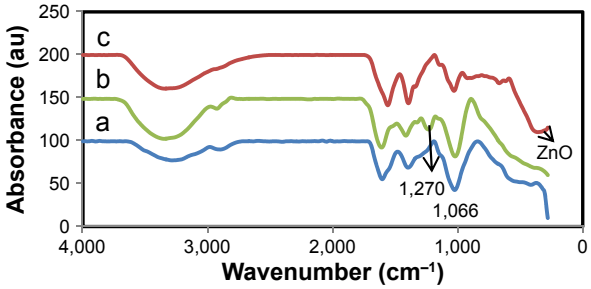

Figure 1 FTIR spectra of (a) hyaluronan, (b) *Sargassum muticum*, and (c) HA/ZnO nanocomposite.
Abbreviations: FTIR, Fourier transform infrared; HA, hyaluronan; ZnO, zinc oxide.

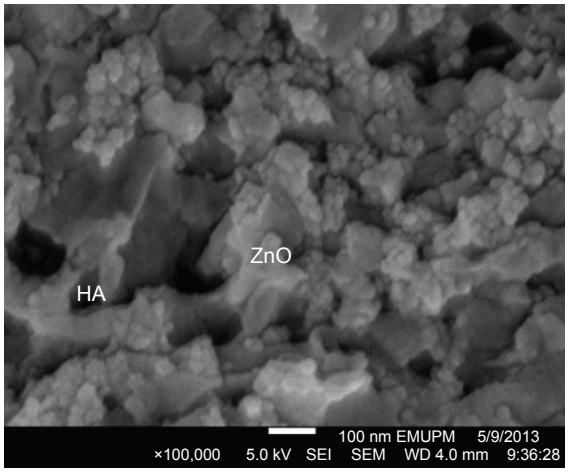

Figure 2 FESEM image of the HA/ZnO nanocomposite.
Abbreviations: FESEM, field emission scanning electron microscopy; HA/ZnO, hyaluronan/zinc oxide.

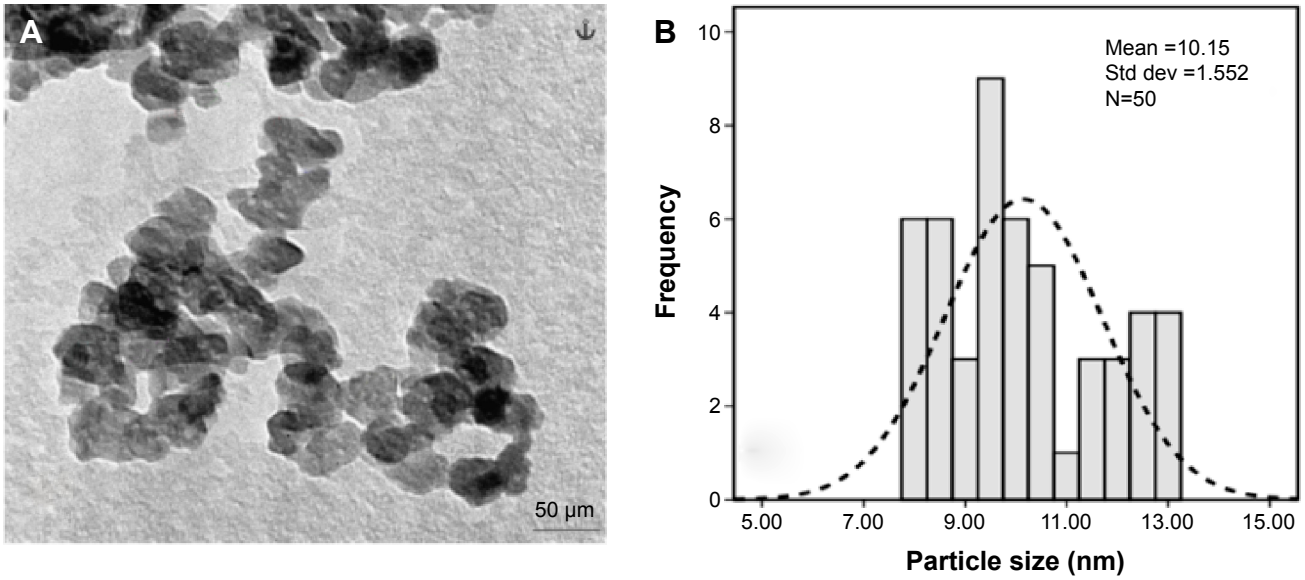

Figure 3 Morphological characteristic of HA/ZnO nanocomposite.
Notes: (**A**) TEM image and (**B**) particle size distribution of the HA/ZnO nanocomposite.
Abbreviations: TEM, transmission electron microscope; HA/ZnO, hyaluronan/zinc oxide; Std dev, standard deviation.

Figure 2 illustrates FESEM image of HA/ZnO nanocomposite. The polygonal shapes of ZnO nanoparticles with a mean diameter of 3–8 nm are evident on the surface of HA. The results are consistent with the firm binding of ZnO nanoparticles to HA, and the formation of this complex inhibits nanoparticle aggregation and agglomeration.

The average particle size and distribution of ZnO nanoparticles were estimated under TEM. The polydispersed ZnO nanoparticles with the hexagonal wurtzite structure are shown in Figure 3A. The size of the nanoparticles is 10.2±1.5 nm (Figure 3B). The TEM image clearly suggests the presence of secondary materials, shown by the dark shadows on the surface of ZnO nanoparticles, which may be the bioorganic molecules of *S. muticum*. The interaction between ZnO nanoparticles and *S. muticum* was confirmed by FTIR (Figure 1).

Figure 4 illustrates the X-ray diffraction pattern of HA/ZnO nanocomposite. The prominent peaks are attributed to the hexagonal wurtzite structure of ZnO (PDF Card: 00-036-1451). Broadening of line and sharpness of the diffraction peaks are evident, indicating that HA/ZnO nanocomposite was not only in nanometer range in size but also crystalline. Using the Debye–Scherrer equation, the diameter of the HA/ZnO nanoparticles was ~12 nm, which is in agreement with TEM and FESEM results.

A sharp absorption peak can be seen at wavelength 344 nm (Figure 5), confirming the direct band gap absorption of ZnO crystals due to the electron transitions from the valence band to the conduction band ($O_{2p} \rightarrow Zn_{3d}$).[24] Thus, the results show that incorporation of ZnO into HA produces nanocomposite with excellent UV light absorbance capacity. The HA/ZnO nanocomposite was stable in solution even after 6 months. The polydispersity of HA and HA/ZnO nanocomposite is shown in Figure 6. The synthesis of HA/ZnO nanoparticles had decreased the size distribution of HA.

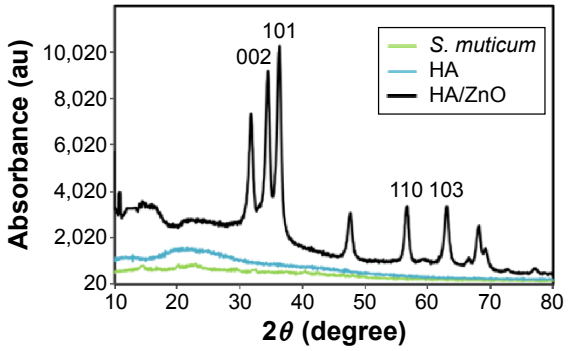

Figure 4 X-ray diffraction pattern of the HA/ZnO nanocomposite.
Abbreviations: HA, hyaluronan; ZnO, zinc oxide; *S. muticum*, *Sargassum muticum*.

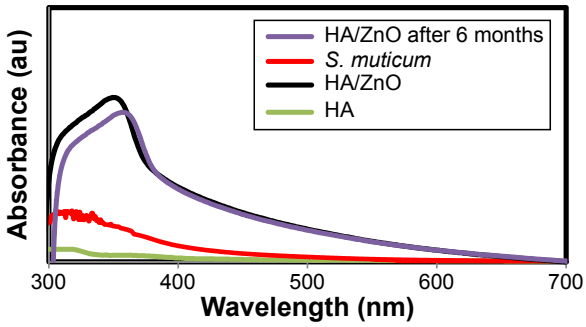

Figure 5 UV–vis absorption spectrum of the HA/ZnO nanocomposite.
Abbreviations: UV, ultraviolet; HA, hyaluronan; ZnO, zinc oxide; *S. muticum*, *Sargassum muticum*.

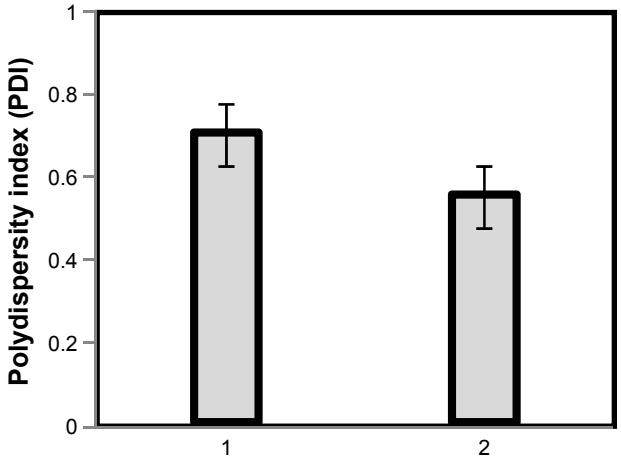

Figure 6 The polydispersity index of the HA (1) and HA/ZnO (2) nanocomposite.
Abbreviations: HA, hyaluronan; ZnO, zinc oxide.

HA/ZnO nanocomposite inhibits proliferation of human cancer cells

The cytotoxicity study showed that HA/ZnO nanocomposite causes morphological changes and inhibits proliferation of cancer cells in dose- and time-dependent manner (Figure 7A). The HA/ZnO was not toxic to normal human lung (MRC-5) cells (Figure 7B). The IC_{50} values of HA/ZnO nanocomposite on cancer cells were 10.8±0.3 µg/mL for PANC-1, 15.4±1.2 µg/mL for CaOV-3, 12.1±0.9 µg/mL for COLO-205, and 6.25±0.5 µg/mL for HL-60 cell lines at 72 hours of treatment. In comparison, the IC_{50} of cisplatin on HL-60 cells was 10±0.5 µg/mL, 1.55±0.73 µg/mL, and 1.3±0.07 µg/mL after 24 hours, 48 hours, and 72 hours treatment, respectively (Figure 7C). The HL-60 cell lines

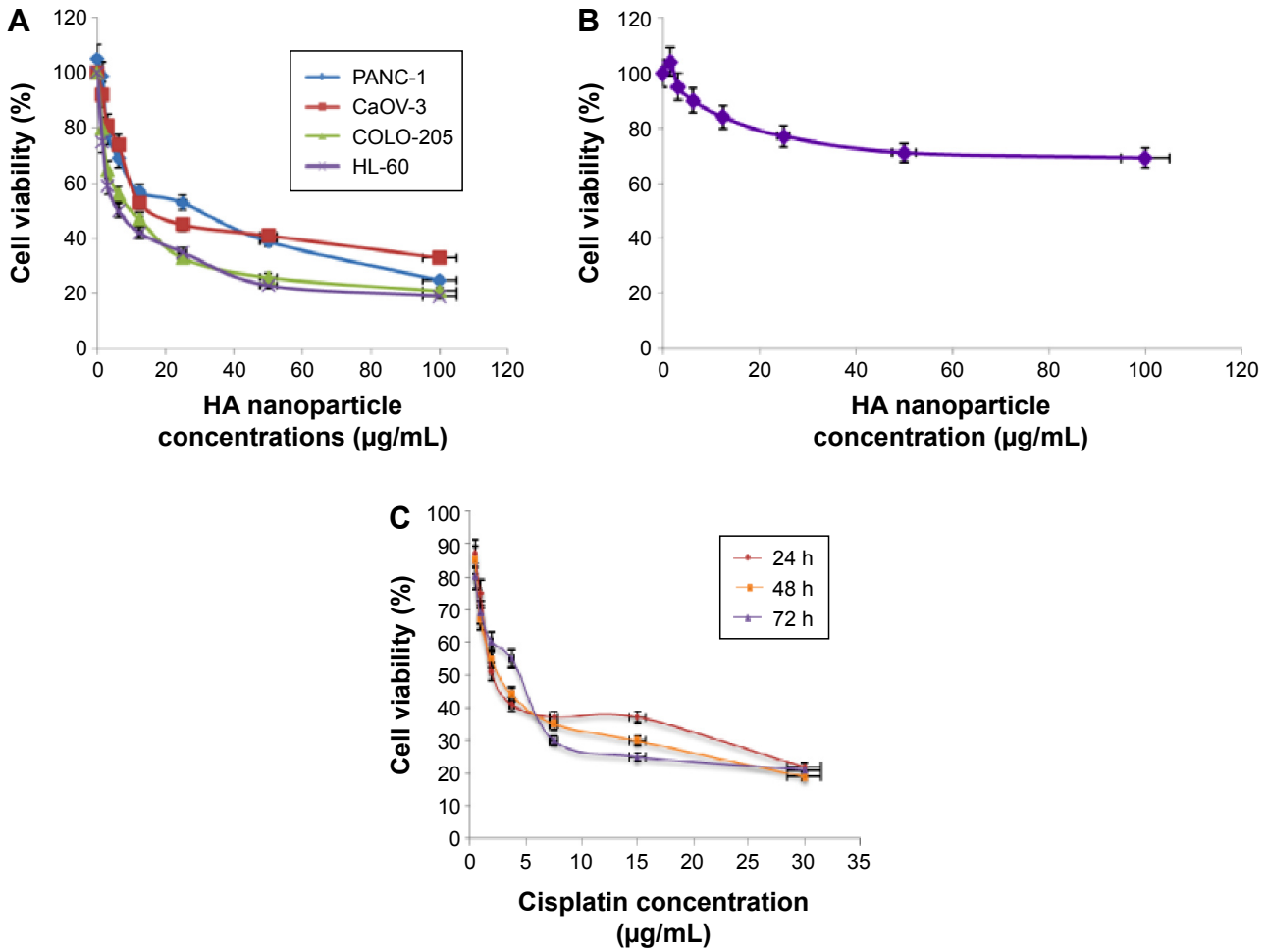

Figure 7 Cytotoxic effect of HA/ZnO nanocomposite and Cisplatin using 3-(4,5-dimethylthiazol-2-yl)-2,5-diphenyltetrazolium bromide on various human cell lines.
Notes: (**A**) Cytotoxic effects of HA/ZnO nanocomposite on various human cancer cells at 72 h of treatment were evaluated using MTT assay. Each point is the mean value of three replicates. PANC-1: pancreatic adenocarcinoma cell line, CaOV-3: ovarian adenocarcinoma cell line, COLO-205: colonic adenocarcinoma cell line, HL-60: acute promyelocytic leukemia cells. (**B**) Cytotoxic effects of HA/ZnO nanocomposite on normal human lung fibroblast cell line (MRC-5) at 72 h of treatment were evaluated using MTT assay. Each point is the mean value of three replicates. (**C**) Cytotoxic effects of cisplatin on HL-60 cells at 24 h, 48 h, and 72 h of treatment were evaluated through mitochondrial activity using the MTT assay. Each point is the mean value of three replicates.
Abbreviations: HA/ZnO, hyaluronan/zinc oxide; h, hours; MTT, 3-(4,5-dimethylthiazol-2-yl)-2,5-diphenyltetrazolium bromide.

were most susceptible to the cytotoxic effect of HA/ZnO nanocomposite.

Quantification of apoptosis using AO/PI double staining

Apoptosis induction is the most sought after effect in cancer therapies. Apoptotic HL-60 cells show several cellular and molecular biological features, such as cell shrinkage, DNA fragmentations, and activation of the caspase cascade with HA/ZnO nanocomposite treatment. The HA/ZnO nanocomposite also inhibited HL-60 growth in time- and dose-dependent manner (Figure 8). Untreated cells show diffuse green fluorescence, while apoptotic cells showed clumps of intense green fluorescent spots suggesting condensed chromatin during apoptosis of the HL-60 cells. There is also characteristic chromatin condensation in periphery of the nucleus shown by crescent shape and numerous round clumps.

Annexin V–fluorescein isothiocyanate assay

Annexin is a family of calcium-dependent phospholipid-binding proteins that binds to externalized phosphatidylserine of cells undergoing apoptosis. This was also evident by flow cytometric analysis of AO/PI-stained HA/ZnO nanocomposite-treated HL-60 cells. The distribution of HA/ZnO nanocomposite-treated cells in early apoptosis and late apoptosis was significantly higher than that for the untreated cells (Figure 9; Table 1). In addition, the HA/ZnO nanocomposite treatment unlike the nontreatment only slightly decreases the population of viable cells.

Cell cycle assay

In cells treated with apoptosis-inducing agents, a subpopulation of cells in sub-G1 phase of the cycle should increase. This is the result of endonuclease activation and subsequent

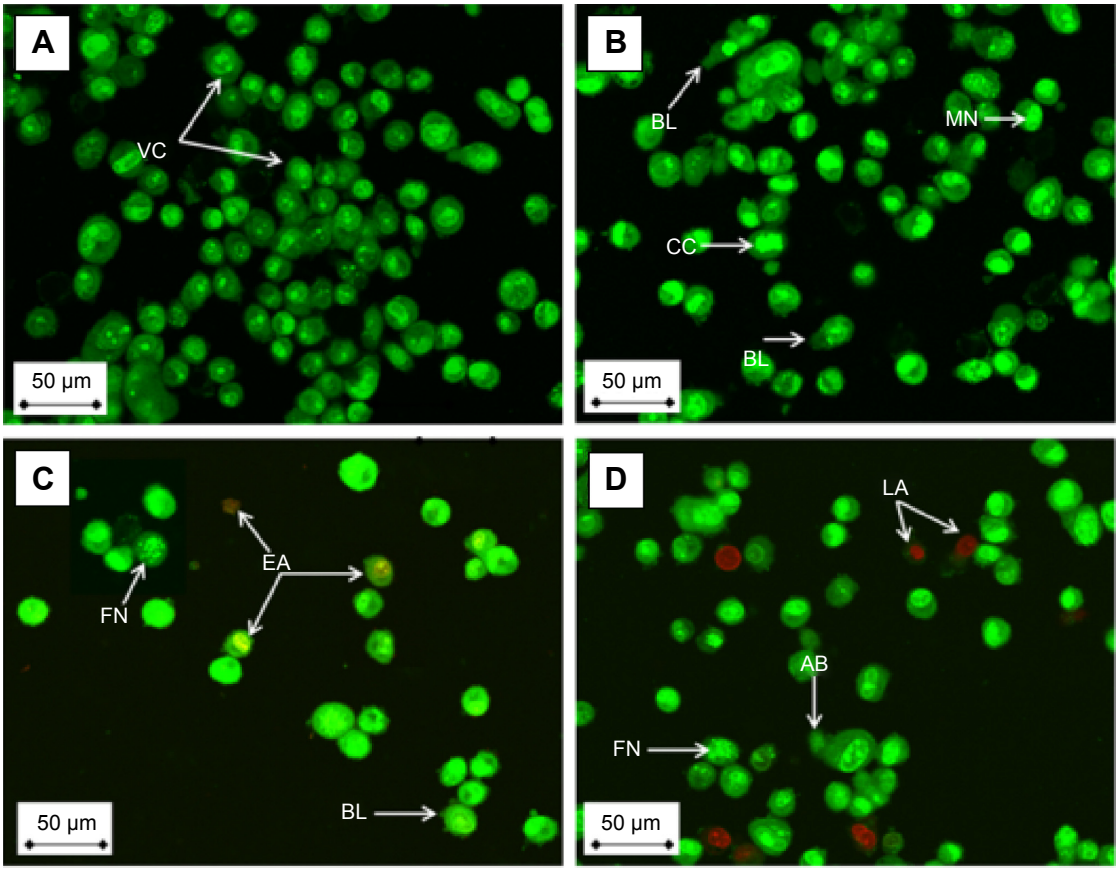

Figure 8 Fluorescent micrograph of AO/PI double-stained HL-60 cells that were treated with HA/ZnO nanocomposite.
Notes: (**A**) Untreated cells showing normal cell structure. (**B**) Treated cells after 24 h showing membrane blebbing, nuclear margination, and chromatin condensation. (**C**) Early apoptotic cells showing blebbing and nuclear fragmentation after 48 h treatment. (**D**) Late apoptotic cells showing nuclear fragmentation and apoptotic body formation after 72 h treatment (magnification 400×).
Abbreviations: AO/PI, acridine orange/propidium iodide; HL-60, acute promyelocytic leukemia cells; HA/ZnO, hyaluronan/zinc oxide; VC, viable cells; BL, membrane blebbing; CC, chromatin condensation; MN, marginated nucleus; EA, early apoptotic cells; FN, fragmented nucleus; LA, late apoptotic cells; AB, apoptotic body.

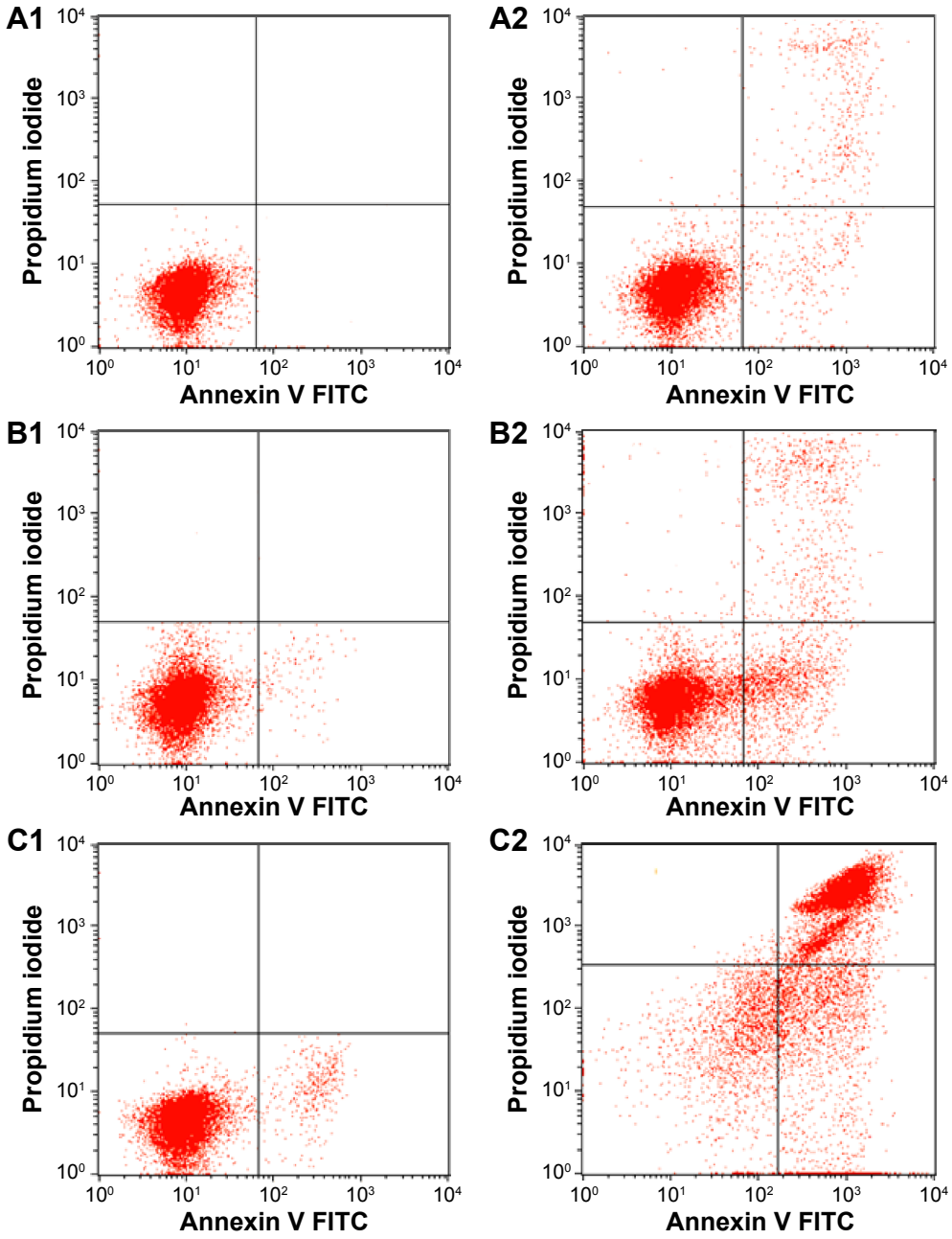

Figure 9 Flow cytometric analysis of apoptosis induction by HA/ZnO nanocomposite in HL-60 cells after staining with FITC-conjugated annexin-V and PI.
Notes: (**A1**–**C1**) Untreated (control) HL-60 cells at 6 h, 12 h, and 24 h incubation, respectively. (**A2**–**C2**) Effects of 6 h, 12 h, and 24 h HA/ZnO nanocomposite treatment, respectively.
Abbreviations: HA/ZnO, hyaluronan/zinc oxide; HL-60, acute promyelocytic leukemia cells; FITC, fluorescein isothiocyanate; PI, propidium iodide; h, hours.

Table 1 Flow cytometric analysis of HL-60 cells treated with HA/ZnO nanocomposite

Cell condition	Cells (%)					
	Control 6 h	Treated 6 h	Control 12 h	Treated 12 h	Control 24 h	Treated 24 h
Viable cells	97.4±0.74	80.29±0.65	92.30±0.55	75.29±0.15	90.7±0.25	73.5±0.13
Early apoptosis	1.87±0.15	10.5±0.99*	4.95±0.70	15.00±0.30*	6.1±0.45	9.5±0.22*
Late apoptosis/necrosis	0.69±0.35	8.65±0.95**	2.62±0.50	10.7±0.80**	3.8±0.25	16.9±0.10**

Notes: The cells were stained with FITC-conjugated annexin-V and PI and incubated at 37°C for 6 h, 12 h, and 24 h. Values are expressed as mean ± SD of three different experiments. Data have been analyzed using post hoc comparison test, one-way ANOVA, and means compared by Tukey's *b*-test. *Significant ($P<0.05$) increase of early apoptotic cells in HA/ZNO nanocomposite-treated groups compared to that of untreated control. **Significant ($P<0.05$) increase of late apoptotic/necrotic cells in HA/ZnO nanocomposite-treated groups compared to that of untreated control.
Abbreviations: HL-60, acute promyelocytic leukemia cells; HA/ZnO, hyaluronan/zinc oxide; h, hours; FITC, fluorescein isothiocyanate; PI, propidium iodide; ANOVA, analysis of variance; SD, standard deviation.

leakage of DNA from the cells. Since necrotic cells do not show the immediate reduction in DNA content, the distinction between apoptotic and necrotic cells can be made. As shown in Figure 10 and Table 2, there is G2/M cell cycle arrest in the HA/ZnO nanocomposite-treated HL-60 cells in a time-dependent manner. The cell population in G2/M phase increased from 16.85%±0.76% to 20.0%±0.41% after 24 hours, from 19.16%±0.26% to 26.29%±0.35% after 48 hours, and from 22.30%±0.22% to 27.06%±0.93% after 72 hours of exposure to HA/ZnO nanocomposite.

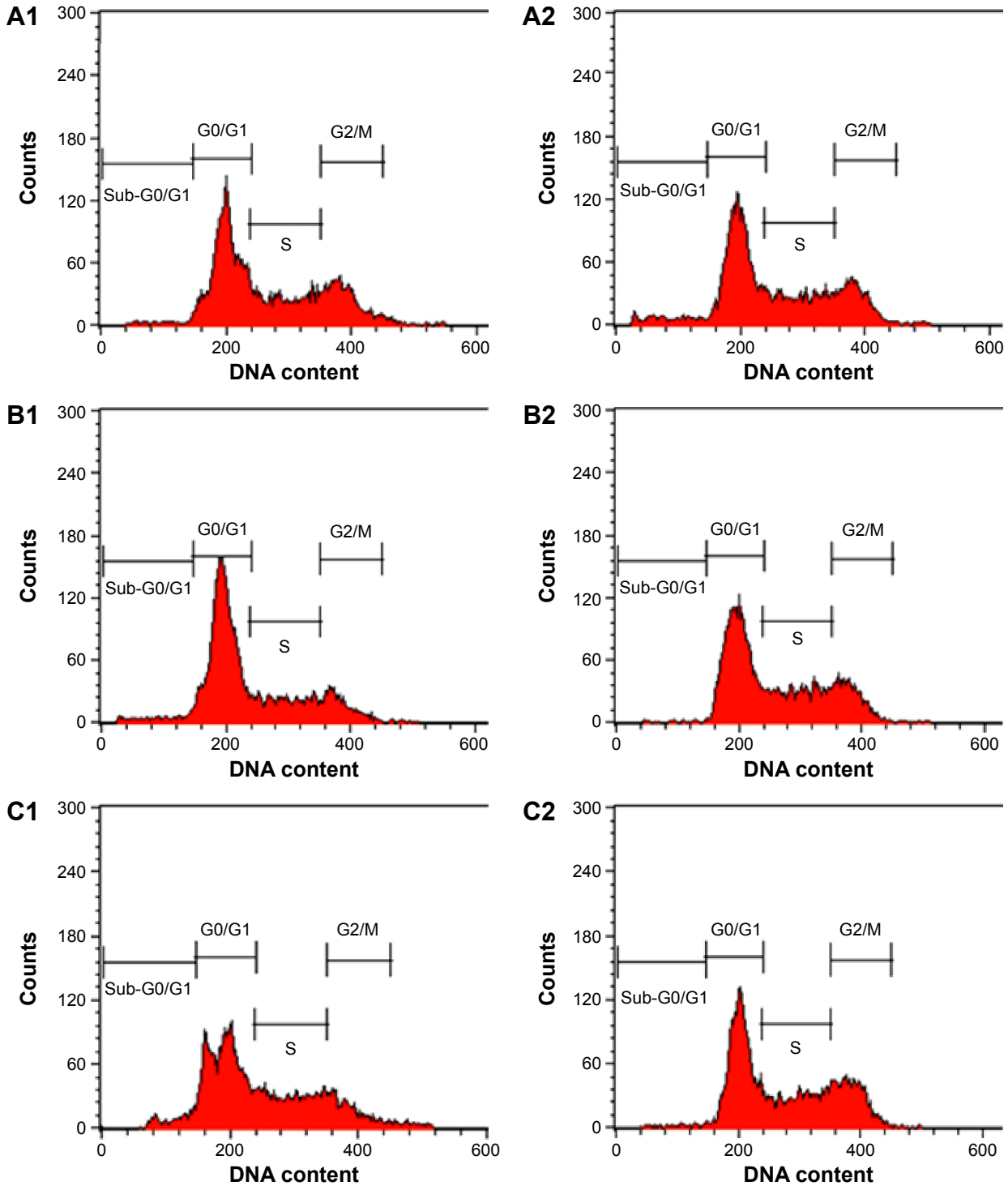

Figure 10 Cell cycle analysis of HL-60 cells treated with HA/ZnO nanocomposite after staining with PI.
Notes: (**A1**–**C1**) Untreated HL-60 cells for 24 h, 48 h, and 72 h, respectively. (**A2**–**C2**) Effects of 24 h, 48 h, and 72 h, respectively, exposure of HL-60 cells to HA/ZnO nanocomposite. G0/G1, G2/M, and S indicate the cell phase, and sub-G0/G1 refers to the portion of apoptotic cells.
Abbreviations: HL-60, acute promyelocytic leukemia cells; HA/ZnO, hyaluronan/zinc oxide; PI, propidium iodide; h, hours.

Table 2 Flow cytometric analysis of HL-60 cells treated with HA/ZnO nanocomposite

Cell cycle phases	Cells (%)					
	Control 24 h	Treated 24 h	Control 48 h	Treated 48 h	Control 72 h	Treated 72 h
G0/G1	55.25±0.06	43.40±0.45	52.10±0.29	42.61±0.52	40.64±0.32	35.68±0.68
G2/M	16.85±0.76	20.00±0.41*	19.16±0.26	26.29±0.35*	22.30±0.22	27.06±0.93*
Synthesis	24.91±0.06	26.30±0.33	26.24±0.06	20.93±0.12	31.50±0.61	25.35±0.18
Sub-G0/G1	1.9±0.23	10.50±0.28*	2.50±0.34	10.00±0.20*	6.20±0.46	13.85±0.56*

Notes: The cells were stained with PI and incubated at 37°C for 24 h, 48 h, and 72 h. Values are expressed as mean ± SD of three different experiments. Data have been analyzed using post hoc comparison test, one-way ANOVA, and means compared by Tukey's *b*-test. *Significant ($P<0.05$) increase of cells in sub-G0/G1 phase with accumulation and G2/M cell cycle arrest in HA/ZNO nanocomposite-treated groups compared to that of untreated control.
Abbreviations: HL-60, acute promyelocytic leukemia cells; HA/ZnO, hyaluronan/zinc oxide; h, hours; PI, propidium iodide; ANOVA, analysis of variance; SD, standard deviation.

The results show that HA/ZnO nanocomposite is potentially an efficacious anticancer agent.

Caspase assay

The induction of apoptosis by HA/ZnO nanocomposite can also be determined by quantitating the activities of caspase-3 and -9 that orchestrate cell death. Caspase-3, -6, and -7 coordinate the execution phase of apoptosis by cleaving multiple structural and repair proteins. Activation of caspase-3 is either dependent on or independent of mitochondrial cytochrome c release and caspase-9 function. In this study, the activity of caspase-3 and -9 was investigated relative to the protein content of cells after treatment with the IC_{50} concentrations of HA/ZnO nanocomposite. The results showed that the activity of caspases increases in a time-dependent manner (Figure 11; Table 3).

Conclusion

The fabrication of HA/ZnO nanocomposite is a simple, safe, and economical procedure. The zinc oxide nanoparticles with a particle size of <13 nm can be incorporated into HA with *S. muticum* in the reaction medium. This nanocomposite as a drug-delivery vehicle allows for high drug uptake and facilitative drug release into tumor while minimal release into normal tissues. This will enhance the therapeutic efficacy of drugs without causing rampant toxicity to normal tissues. These properties of the HA/ZnO nanocomposite can easily be translated into an efficacious therapeutic anticancer drug delivery system with potential for cancer tissue targeting.

Acknowledgments

The authors are grateful to the staff of Universiti Putra Malaysia, especially those of the UPM-MAKNA-Cancer

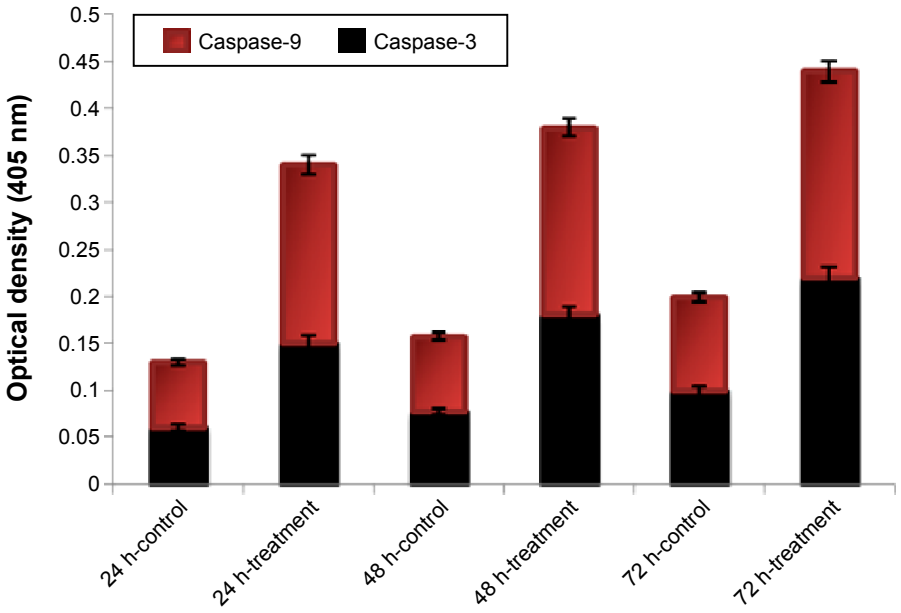

Figure 11 Effects of HA/ZnO nanocomposite treatment on HL-60 cell caspase-3 and -9.
Notes: The values are mean ± SD of three independent experiments. Significant differences ($P<0.05$) between treated and control groups for caspase-3 and -9 are found.
Abbreviations: HA/ZnO, hyaluronan/zinc oxide; HL-60, acute promyelocytic leukemia cells; h, hours; SD, standard deviation.

Table 3 Caspases spectrophotometric analysis of HL-60 cells treated with HA/ZnO nanocomposite for 24 h, 48 h, and 72 h

Caspase	Cells (%)					
	Control 24 h	Treated 24 h	Control 48 h	Treated 48 h	Control 72 h	Treated 72 h
Caspase-3	0.060±0.0012	0.15±0.001*	0.077±0.005	0.18±0.0043*	0.099±0.0032	0.22±0.006*
Caspase-9	0.069±0.007	0.19±0.003*	0.080±0.001	0.20±0.0025*	0.12±0.002	0.24±0.0035*

Notes: Values are expressed as mean ± SD of three different experiments. Data have been analyzed using post hoc comparison test, one-way ANOVA, and means compared using Tukey's *b*-test. *Significant ($P<0.05$) increase of apoptotic cells in HA/ZnO nanocomposite-treated groups compared to that of untreated control.
Abbreviations: HL-60, acute promyelocytic leukemia cells; HA/ZnO, hyaluronan/zinc oxide; h, hours; ANOVA, analysis of variance; SD, standard deviation.

Research Laboratory, Institute of Bioscience, for their cooperation and technical assistance.

Disclosure

The authors report no conflicts of interest in this work.

References

1. Roy M, Nelson JK, MacCrone RK, Schadler LS, Reed CW, Keefe R. Polymer nanocomposite dielectrics-the role of the interface. *IEEE Trans Dielectr Electr Insul*. 2005;12(4):629–643.
2. Hariraksapitak P, Supaphol P. Preparation and properties of α-chitin whisker-reinforced hyaluronan–gelatin nanocomposite scaffolds. *J Appl Polym Sci*. 2010;117(6):3406–3418.
3. Chong BF, Blank LM, Mclaughlin R, Nielsen LK. Microbial hyaluronic acid production. *Appl Microbiol Biotechnol*. 2005;66(4):341–351.
4. Pecharki D, Petersen FC, Scheie AA. Role of hyaluronidase in *Streptococcus intermedius* biofilm. *Microbiology*. 2008;154(3):932–938.
5. Armstrong DC, Johns MR. Culture conditions affect the molecular weight properties of hyaluronic acid produced by *Streptococcus zooepidemicus*. *Appl Environ Microbiol*. 1997;63:2759–2764.
6. Asteriou T, Deschrevel B, Delpech B, et al. An improved assay for the N-Acetyl-d-glucosamine reducing ends of polysaccharides in the presence of proteins. *Anal Biochem*. 2001;293(1):53–59.
7. Liu L, Du G, Chen J, Zhu Y, Wang M, Sun J. Microbial production of low molecular weight hyaluronic acid by adding hydrogen peroxide and ascorbate in batch culture of *Streptococcus zooepidemicus*. *Bioresour Technol*. 2009;100(1):362–367.
8. Duan XJ, Niu HX, Tan WS, Zhang X. Mechanism analysis of effect of oxygen on molecular weight of hyaluronic acid produced by *Streptococcus zooepidemicus*. *J Microbiol Biotechnol*. 2009;19(3):299–306.
9. Lai ZW, Rahim RA, Ariff AB, Mohamad R. Biosynthesis of high molecular weight hyaluronic acid by *Streptococcus zooepidemicus* using oxygen vector and optimum impeller tip speed. *J Biosci Bioeng*. 2012;114(3):286–291.
10. Rozenberg BA, Tenne R. Polymer-assisted fabrication of nanoparticles and nanocomposites. *Prog Polym Sci*. 2008;33(1):40–112.
11. Arockiya Aarthi Rajathi F, Parthiban C, Ganesh Kumar V, Anantharaman P. Biosynthesis of antibacterial gold nanoparticles using brown alga, *Stoechospermum marginatum* (kützing). *Spectrochimica Acta A Mol Biomol Spectrosc*. 2012;99:166–173.
12. Namvar F, Suhaila M, Fard SG, Behravan J. Polyphenol-rich seaweed (*Eucheuma cottonii*) extract suppresses breast tumour via hormone modulation and apoptosis induction. *Food Chem*. 2012;130:376–382.
13. Wada K, Nakamura K, Tamai Y, et al. Seaweed intake and blood pressure levels in healthy pre-school Japanese children. *Nutr J*. 2011;10(1):83.
14. Rahman HS. *Anti-Leukemic Effects of Zerumbone Nanoparticle on Human Jurkat T Lymphoblastoid Cell Lines In Vitro and Murine Leukemic WEHI-3B Model In Vivo*. Kuala Lumpur: University Putra Malaysia; 2014.
15. Merisko-Liversidge EM, Liversidge GG. Drug nanoparticles: formulating poorly water-soluble compounds. *Toxicol Pathol*. 2008;36(1):43–48.
16. Rahman HS, Rasedee A, Chee WH, et al. Zerumbone loaded nanostructured lipid carriers: preparation, characterization and antileukemia effect. *Int J Nanomed*. 2013;8:2769–2781.
17. Rahman HS, Abdullah R, Ahmad BA, et al. Zerumbone-loaded nanostructured lipid carrier induces G2/M cell cycle arrest and apoptosis via mitochondrial pathway in human lymphoblastic leukemia cell line. *Int J Nanomed*. 2014;9:527–538.
18. Hosseinpour M, Abdul AB, Rahman HS, et al. Comparison of apoptotic inducing effect of zerumbone and zerumbone-loaded nanostructured lipid carrier on human mammary adenocarcinoma MDA-MB-231 cell line. *J Nanomater*. 2014;2014:10.
19. Rahman HS, Rasedee A, Chee WH, et al. Antileukemic effect of zerumbone-loaded nanostructured lipid carrier on murine leukemic (WEHI-3B) model. *Int J Nanomed*. 2015;10:1649.
20. Donghui F, Beibei W, Zheng X, Qisheng G. Determination of hyaluronan by spectroscopic methods. *J Wuhan Univ Technol Mater Sci Ed*. 2006;21(3):32–34.
21. Venkatpurwar V, Pokharkar V. Green synthesis of silver nanoparticles using marine polysaccharide: study of in-vitro antibacterial activity. *Mater Lett*. 2011;65(6):999–1002.
22. Azizi S, Ahmad MB, Namvar F, Mohamad R. Green biosynthesis and characterization of zinc oxide nanoparticles using brown marine macroalga *Sargassum muticum* aqueous extract. *Mater Lett*. 2014;116:275–277.
23. Barros Gomes Camara R, Silva Costa L, Pereira Fidelis G, et al. Heterofucans from the brown seaweed *Canistrocarpus cervicornis* with anticoagulant and antioxidant activities. *Mar Drugs*. 2011;9(1):124–138.
24. Azizi S, Ahmad MB, Mahdavi M, Abdolmohammadi S. Preparation, characterization, and antimicrobial activities of ZnO nanoparticles/cellulose nanocrystal nanocomposites. *BioResource*. 2013;8(2):1841–1851.